RSC Advances

PAPER

Cite this: *RSC Adv.*, 2024, **14**, 4456

Design of N–N ylide bond-based high energy density materials: a theoretical survey†

Jingfan Xin, *[a] Xiaoxu Bo,[b] Wenmin Xiao,[a] Yihong Ding, *[cd] Ruifa Jin *[a] and Suhua Yang[a]

The generally encountered contradiction between large energy content and stability poses great difficulty in designing nitrogen-rich high-energy-density materials. Although N–N ylide bonds have been classified as the fourth type of homonuclear N–N bonds (besides >N–N<, –N=N–, and N≡N), accessible energetic molecules with N–N ylide bonds have rarely been explored. In this study, 225 molecules with six types of novel structures containing N–N ylide bonds were designed using density functional theory and CBS-QB3 methods. To guide future synthesis, the effects of substitution on the thermal stability, detonation velocity, and detonation pressure of the structures were evaluated under the premise that the N–N ylide skeleton remains stable. The calculations show that the bond dissociation energy values of the N–N ylide bonds of the designed 225 structures were in the range of 61.21–437.52 kJ mol^{-1}, except for N-^{1}NNH$_2$. Many of the designed structures with N–N ylide bonds exhibit high detonation properties, which are superior to those of traditional energetic compounds. This study convincingly demonstrates the feasibility of the design strategy of introducing an N–N ylide bond to develop new types of energetic materials.

Received 23rd December 2023
Accepted 19th January 2024

DOI: 10.1039/d3ra08799a

rsc.li/rsc-advances

1. Introduction

High energy density materials (HEDMs) play an important role in military and civil fields.[1–6] Finding an ideal HEDM molecule is always an extraordinary challenge due to the great difficulty in achieving the intrinsic requirements, *i.e.*, structural stability (to allow safe usage) and large energy release (to ensure excellent detonation properties). It is known that among the known N–N bond-containing non-salt-like high-energy materials, the N–N bonds in the skeleton structure mostly take the form of N–N single or double bonds. This is due to the large energy difference between the N–N single bond (~160 kJ mol^{-1}), double bond (~420 kJ mol^{-1}), and triple bond (close to 1 MJ mol^{-1}), which means that there is a higher energy release, meeting the requirements of candidate energetic materials.[7,8]

Among the known N–N bond-containing HEDM compounds (Scheme 1), the skeletal N–N bond mostly takes the normal N–N single or double bonding forms. The N–N ylide bond is the fourth homonuclear N–N bond, and the other three normal N–N key types are >N–N<, –N=N–, and N≡N. Since the first report of synthesis in the 1950s,[9] the N–N ylide family has grown into two known structural types, *i.e.*, the pyridine type (sp^2 type) and the aminimide type (sp^3 type).[10–12] Due to their zwitterionic properties, they exhibit unique physicochemical properties and are therefore widely used in a variety of applications, such as polymer additives in binders and surfactants.[13,14] In recent years, the development of more concise and efficient methods for the generation and application of N–N ylide to synthesize highly functional compounds has been of great interest.[15–17] The bond energy of the N–N ylide bond is similar to that of an N–N single bond, which is very advantageous as a high-energy

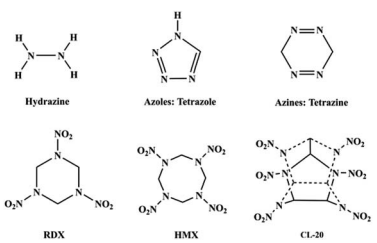

Scheme 1 Some known HEDMs containing normal N–N single or double bonds. Hydrogen atoms attached to carbon are not shown.

[a]*Inner Mongolia Key Laboratory of Photoelectric Functional Materials, College of Chemistry and Life Science, Chifeng University, Chifeng 024000, China. E-mail: xinjingfan25@163.com*

[b]*Department of Agriculture and Biotechnology, Wenzhou Vocational College of Science and Technology, No. 1000 Liuhongqiao Road, Wenzhou 325006, People's Republic of China*

[c]*Key Laboratory of Carbon Materials of Zhejiang Province, Wenzhou Key Lab of Advanced Energy Storage and Conversion, Zhejiang Province Key Lab of Leather Engineering, College of Chemistry and Materials Engineering, Wenzhou University, Wenzhou 325035, P. R. China*

[d]*Laboratory of Theoretical and Computational Chemistry, Institute of Theoretical Chemistry, Jilin University, Changchun, China*

† Electronic supplementary information (ESI) available. See DOI: https://doi.org/10.1039/d3ra08799a

structure. However, skeleton structures with N–N ylide bonds have barely been investigated in the high energy density material field. The successful synthesis of new types of energetic compounds with N–O ylide bonds in recent years[18–21] has greatly increased our confidence in the introduction of N–N ylide bond-containing structures into the field of energetic materials.

In this work, we report a novel class of skeleton energetic structures, *i.e.*, N–N ylide bond-based structures. Six types of structures were designed with different substitution effects, leading to 225 molecules in total. A thorough study of their thermal stability and detonation properties showed that appropriate substitution effects can provide both structural thermal stability and energy enrichment, satisfying the ever-challenging and severe criteria of stability and detonation. Our work exemplifies for the first time that structures with the N–N ylide bond can act as promising HEDMs. This work opens up a new avenue for energetic compounds, namely HEDMs, with a fourth type of homonuclear N–N bond, *i.e.*, the N–N ylide bond.

2. Computational methods

The density functional theory method (DFT) is a powerful tool for studying the structures and energetic properties of energetic materials.[22–24] The electronic structures, heats of formation, thermal stabilities, and impact sensitivities were studied by DFT using the Gaussian 09 (ref. 25) program packages. For energy refinement, the composite CBS-QB3 method[26] was applied; the B3LYP/6-311G(2d,d,p) geometries and frequencies were used, followed by a series of high-level single-point energy calculations.

The bond dissociation energies (BDE) of the designed structures were calculated using the following equations.[27]

$$\mathrm{BDE}(A\text{–}B) = E(A\cdot) + E(B\cdot) - E(A\text{–}B) \quad (1)$$

where BDE(A–B) is the BDE of A–B at the CBS-QB3 (0 K) level; $E(A\cdot)$, $E(B\cdot)$, and $E(A\text{–}B)$ are the total energies of $A\cdot$, B, and A–B, respectively.

The heat of formation in the gas phase ($\Delta H_{f,gas}$) was determined using the atomization equation. The known enthalpies of formation of N(g), H(g), O(g), and C(g) were taken from the NIST Chemistry Webbook.[28]

To estimate the detonation performance of the title compounds, their solid-phase heats of formation ($\Delta H_{f,solid}$) were calculated. According to Hess's law,[29,30] $\Delta H_{f,solid}$ can be obtained by

$$\Delta H_{f,solid} = \Delta H_{f,gas} - \Delta H_{sub} \quad (2)$$

where the predicted heat of sublimation (ΔH_{sub}) is represented as shown below in eqn (3), as given by Rice *et al.*[31]

$$\Delta H_{sub} = \alpha A^2 + \beta(\nu\sigma_{total}{}^2)^{1/2} + \gamma \quad (3)$$

where A is the surface area of the isosurface of the 0.001 electrons per Bohr^3 electronic density, ν is the degree of balance between the positive and negative potentials on the isosurface; $\sigma_{total}{}^2$ is a measure of the variability of the electrostatic potential; the coefficients α, β, and γ were determined to be $\alpha = 11.17 \times 10^{-4}$ kJ mol^{-1} A^{-4}, $\beta = 6.90$ kJ mol^{-1}, and $\gamma = 12.41$ kJ mol^{-1}. The computational procedures proposed by Bulat *et al.*[32] were used to compute the descriptors A, ν, and $\sigma_{total}{}^2$. The related data in the equation (*i.e.* A, ν, and $\sigma_{total}{}^2$) were calculated using Lu's procedure.[33]

The detonation velocity (D in km s^{-1}) and detonation pressure (P in GPa) of the title compounds were estimated using eqn (4) and (5).[34]

$$D = 1.01(N\bar{M}^{0.5}Q^{0.5})^{0.5}(1 + 1.3\rho) \quad (4)$$

$$P = 1.558\rho^2 N\bar{M}^{0.5}Q^{0.5} \quad (5)$$

where N is the number of moles of gas produced per gram of explosive and $\bar{M}$ is the mean molecular weight of the gaseous detonation products. Q is the heat of detonation (cal g^{-1}), and it equals the negative of the enthalpy change ΔH during the reaction. ρ is the density of the explosive (g cm^{-3}). To obtain the theoretical density, we applied the improved equation proposed by Politzer *et al.*,[35] according to which the interaction index $\nu\sigma_{tot}{}^2$ is:

$$\rho = \alpha\left(\frac{M}{V(0.001)}\right) + \beta\nu(\sigma_{tot}{}^2) + \gamma \quad (6)$$

where M is the molecular mass (g mol^{-1}) and $V(0.001)$ is the volume of the 0.001 electrons Bohr^3 contour of the electronic density of the molecule (cm^3 per molecule). The coefficients α, β, and γ were 0.9183, 0.0028, and 0.0443, respectively.

3. Results and discussion

3.1 Optimized structures

The simplest form of the N–N ylide bond structure is H_3N–NH, which is an isomer of the energetic structure H_2N–NH_2. In order to prevent the transfer of H over H_3N^+–, the N–N ylide bond is broken. Six types of N–N ylide bond skeleton structures were designed to maintain the N–N ylide bond type by using rigid five- and six-membered ring structures. For ease of discussion, these six N–N ylide-type structures are categorized as pyridine type (sp^2 type) and aminimide type (sp^3 type) (Fig. 1).

In the six optimized types of N–N ylide bond skeleton structures, the bond length of the N–N ylide bond was between

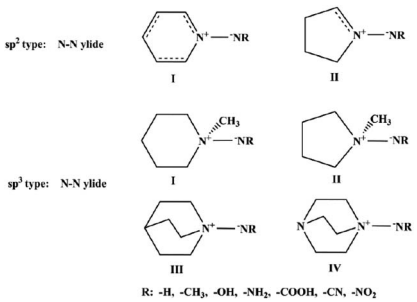

Fig. 1 Design of the six types of structures.

1.30 and 1.44 Å, which is slightly shorter than that of H_3NNH (1.46 Å) and longer than that of the classical N–N double bond (1.24 Å). Further, Mayer bond order calculations showed that the N–N ylide bond can be considered a single bond. The highest occupied orbital (HOMO) and lowest unoccupied orbital (LUMO) of the six types of N–N ylide bond skeleton structures were calculated, and their electronic properties were analyzed. The HOMO–LUMO orbitals of the N–N ylide bond skeleton structures (R = H) are shown in Fig. 2. The HOMO–LUMO gap ranged from 4.17 to 4.80 eV, which is larger than that of H_3NNH (3.81 eV), indicating that these structures can be considered thermodynamically stable (see Table 1 and Fig. 2).

For future experimental synthesis, the substitution effects of different groups were calculated. Selected representative energetic substituted groups, *i.e.*, $-CH_3$, $-OH$, $-NH_2$, $-COOH$, $-CN$, and $-NO_2$, were used to replace H of –NH in the N–N ylide bonds. Meanwhile, CH with N in the five- and six-membered ring rigid skeletons was replaced by an isoelectronic body. The purpose of this study is to explore the influence of substituents on structural thermal stability and energetic properties. A total of 225 structures containing N–N ylide bonds with the functional group and isoelectronic substitutions were optimized at the B3LYP/6-31G(2d,d,p) level. The cartesian coordinates of the optimized structures, bond lengths, and bond dissociation energies of the N–N ylide bonds in all these structures are listed in the ESI (Tables S1–S3).†

3.2 Bond dissociation energies

Bond dissociation energies (BDE) provide useful information regarding the thermal stability of structures.[27,28] The higher the BDE, the better the thermal stability. The calculated BDEs of the N–N ylide bonds of the 225 designed structures are listed in Table S3.† Their BDE values were found to be in the range from 61.21 to 437.52 kJ mol^{-1}, except for N-$^1NNH_2$. In general, the structures substituted with electron-withdrawing groups have larger BDEs than those substituted with electron-donating groups, which might indicate higher thermal stability.

3.3 Detonation performance

It is well known that ideal energetic materials not only require high thermal conductivity but also must exhibit excellent detonation performance (density $\rho \approx 1.9$ g cm^{-3}, detonation velocity $D \approx 9.0$ km s^{-1}, and $P \approx 40.0$ GPa). For comparison, the properties of known species, such as 2,4,6-trinitrotoluene (TNT), 1,3,5-trinitro-1,3,5-triazinane (RDX), and 1,3,5,7-tetranitro-1,3,5,7-tetrazocane (HMX), are also provided. The heats of formation, crystal density (ρ), detonation velocity (D), and detonation pressure (P) of the 225 structures were calculated, and the results are listed in Table S4.†

Table 1 Bond length (Å), Mayer bond indices, highest Occupied molecular orbital (HOMO), lowest unoccupied molecular orbital (LUMO), and HOMO–LUMO gaps (ΔE) (eV) of the six types of N–N ylide bond skeleton structures (R=H) designed at the B3LYP/6-311G(2d,d,p) level

	Bond length	Bond index	HOMO	LUMO	ΔE
sp^2-I	1.31	1.28	−5.16	−0.99	4.17
sp^2-II	1.30	1.32	−4.96	−0.16	4.80
sp^3-I	1.44	0.95	−3.86	0.66	4.52
sp^3-II	1.43	0.97	−3.87	0.49	4.36
sp^3-III	1.43	0.97	−3.84	0.36	4.20
sp^3-IV	1.43	0.97	−3.95	0.40	4.35
H_3NNH	1.46	0.95	−3.88	−0.07	3.81
N_2H_4	1.49	0.97	−5.59	1.07	6.66
N_2H_2	1.24	1.89	−6.63	−1.56	5.07

The solid-phase heats of formation ($\Delta H_{f,solid}$) of the 225 structures are shown in Fig. 3. All structures were found to have positive heat of formation values from 28.94 kJ mol^{-1} to 1276.21 kJ mol^{-1}. In each type of structural skeleton, the heat of formation was higher as the number of isoelectronic bodies (N) increased (see Fig. 3).

The ρ values of all the designed structures are shown in Fig. 4. In each type of structural skeleton, the ρ value increased as the number of isoelectronic bodies (N) increased. In general, among molecules with the same skeleton structure but different

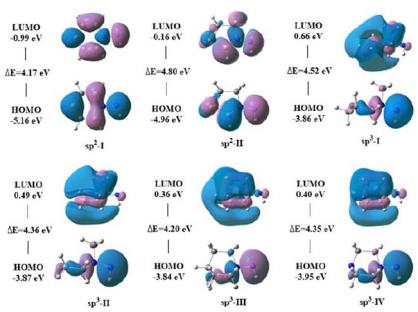

Fig. 2 HOMO–LUMO orbitals and HOMO–LUMO gaps of the six types of N–N ylide bond skeleton structures (R=H) at the B3LYP/6-311G(2d,d,p) level.

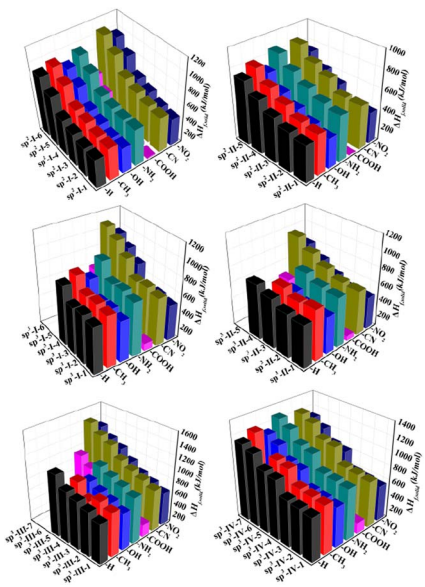

Fig. 3 Heat of formation ($\Delta H_{f,solid}$) (kJ mol^{-1}) of 225 structures.

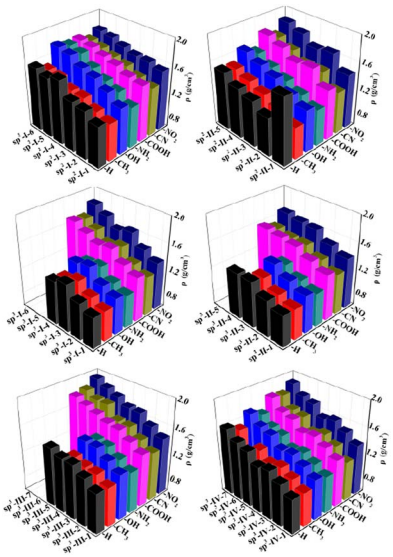

Fig. 4 Crystal density ρ (g cm^{-3}) of the 225 structures.

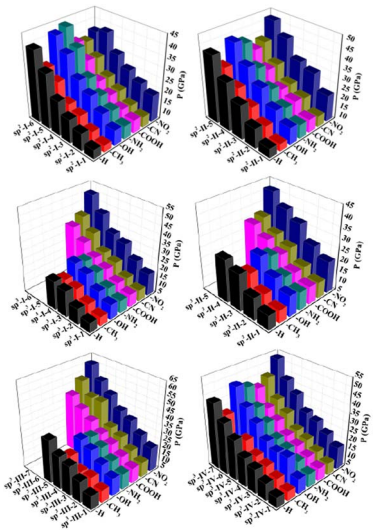

Fig. 6 Detonation pressure P (GPa) of the 225 structures.

substituents, the densities of the electron-withdrawing-group-substituted structures were greater than those of the electron-donating-group-substituted structures.

The detonation velocity and detonation pressure are extremely important for the detonation performance of energetic materials. The D values of all 225 designed structures were found to be between 5.25 and 11.43 km s^{-1}, whereas the P values of all 225 designed structures were found to be from 9.19 to 60.64 GPa. Among them, sp^3-III-7 (R = –NO$_2$) has the highest detonation performance, while sp^2-I-1(R = –CH$_3$) has the lowest detonation performance. In each type of structural skeleton, the detonation velocity and detonation pressure increased with the number of isoelectronic bodies (N) (see Fig. 5 and 6). In general, among molecules of the same structural type but with different substituents, the electron-withdrawing-group-substituted structures (R = –NO$_2$) has higher detonation velocity and detonation pressure, whereas the electron-donating substituted structure (R = –CH$_3$) has lower detonation velocity and detonation pressure.

Thus, quite promisingly, with an increase in N content in the skeleton structure, the structures containing the N–N ylide bond exhibit much better $\Delta H_{f,solid}$, ρ, D, and P values while retaining appreciable thermal stability. On comparing with the calculated substitution effect, it is found that the structures substituted with electron-withdrawing groups have higher detonation performances than those with electron-donating substituents.

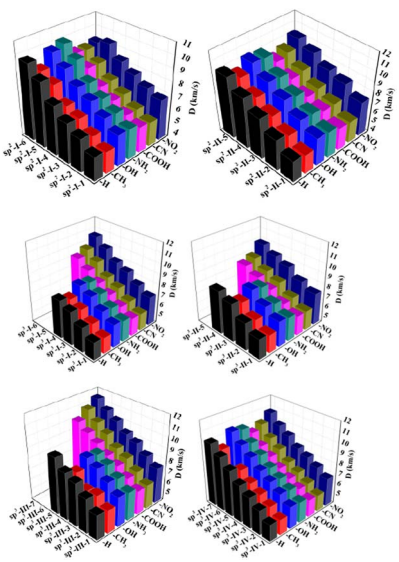

Fig. 5 Detonation velocity D (km s^{-1}) of the 225 structures.

4. Conclusions

In this study, we designed six types of N–N ylide bond-based energetic structures. To ensure thermal stability and detonation properties, different types of substituents (substituent effect) and N content regulation (isoelectronic substitution) in the skeleton structure were employed to obtain 225 structures. In general, the results reveal that the electron-withdrawing-group substitution effect is more beneficial to thermal stability and detonation properties. In addition, the detonation properties of each type of N–N ylide bond-based skeleton structure improve with increasing N content, and some even exceed the values of classical energetic structures. The six types of N–N ylide bond-based structures designed in this work possess excellent thermal stability and detonation properties. Among them, sp^3-III-7 (R = –NO$_2$) has the highest detonation properties (D, P). The combination of the thermal stability and detonation properties suggests that the designed six types of N–N ylide bond-based structures are metastable HEDM candidates worthy of further investigation.

Author contributions

X. J. investigated and wrote the original manuscript. D. Y. wrote programs for detonation properties, guided the entire research,

and reviewed and edited the draft. B. X. and X. W. analysed or synthesized the study data. J. R. provided the servers and software for the calculations. Y. S. collected the data.

Conflicts of interest

There are no conflicts to declare.

Acknowledgements

This work was funded by the Natural Science Foundation of the Inner Mongolia Autonomous Region (No. 2023LHMS02009, 2021LHMS02001, 2023LHMS02013) and the Research Program of Sciences at the Universities of the Inner Mongolia Autonomous Region (No. NJZY21124, NJZY21133, NJZY22192). Y.H. Ding thanks the funding from the National Natural Science Foundation of China (No. 22073069, 21773082).

References

1 Q. Lang, Q. Sun, Q. Wang, Q. H. Lin and M. Lu, *J. Mater. Chem. A*, 2020, **8**, 11752–11760.
2 J. Singh, R. J. Staples and J. M. Shreeve, *ACS Appl. Mater. Interfaces*, 2021, **13**, 61357–61364.
3 J. Singh, R. J. Staples and J. M. Shreeve, *J. Mater. Chem. A*, 2023, **11**, 12896–12901.
4 X. Y. Yang, R. Ahuja and W. Luo, *Nano Energy*, 2023, **113**, 108557–108566.
5 E. Thimsen, *J. Phys. Chem. C*, 2023, **127**, 6601–6609.
6 S. Banik, V. D. Ghule and S. Dharavath, *Mater. Chem. Phys.*, 2023, **301**, 127678–127686.
7 X. H. Jin, F. Yuan, Y. Shen, Y. F. Liu, S. N. Yao, S. C. Bai and B. C. Hu, *J. Phys. Org. Chem.*, 2023, **36**, e4469.
8 A. A. Larin, D. D. Degtyarev, I. V. Ananyev, A. N. Pivkina and L. L. Fershtat, *Chem. Eng. J.*, 2023, **470**, 144144–144154.
9 S. Wawzonek and D. Meyer, *J. Am. Chem. Soc.*, 1954, **76**, 2918–2920.
10 J. A. Pople, K. Raghavachari, M. J. Frisch, J. S. Binkley and P. v. R. Schleyer, *J. Am. Chem. Soc.*, 1983, **105**, 6389–6398.
11 S. L. Jain, V. B. Sharma and B. Sain, *Tetrahedron Lett.*, 2003, **44**, 4385–4387.
12 M. Ochiai, Y. Kawano, T. Kaneaki, N. Tada and K. Miyamoto, *Org. Lett.*, 2009, **11**, 281–284.
13 J. J. Mousseau, J. A. Bull and A. B. Charette, *Angew. Chem., Int. Ed.*, 2010, **49**, 1115–1118.
14 L. Maestre, R. Dorel, Ó. Pablo, I. Escofet, W. M. C. Sameera, E. Álvarez, F. Maseras, M. M. Díaz-Requejo, A. M. Echavarren and P. J. Pérez, *J. Am. Chem. Soc.*, 2017, **139**, 2216–2223.
15 H. G. Im, W. J. Choi and S. Hong, *Angew. Chem., Int. Ed.*, 2020, **132**, 17664–17669.
16 M. M. Xu, W. B. Cao, X. P. Xu and S. J. Ji, *Adv. Synth. Catal.*, 2022, **364**, 2211–2220.
17 W. Lee, Y. Koo, H. Jung, S. Chang and S. Hong, *Nat. Chem.*, 2023, **15**, 1091–1099.
18 D. E. Chavez, D. A. Parrish, L. Mitchell and G. H. Imler, *Angew. Chem., Int. Ed.*, 2017, **56**, 1–5.
19 C. M. Ma, Y. Pan, J. C. Jiang, Z. L. Liu and Q. Z. Yao, *New J. Chem.*, 2018, **42**, 11259–11263.
20 J. Li, Y. B. Liu, W. Q. Ma, T. Fei, C. L. He and S. P. Pang, *Nat. Chem.*, 2022, **13**, 5697–5713.
21 R. Z. Gilmanov, V. G. Nikitin, F. G. Khayrutdinov, K. V. Strizhenko, K. Yu. Suponitsky and A. B. Sheremetev, *Mendeleev Commun.*, 2022, **32**, 114–116.
22 Q. Lang, Q. H. Lin, P. C. Wang, Y. G. Xu and M. Lu, *Front. Chem.*, 2022, **10**, 993036–993045.
23 A. V. Makarenkov, S. S. Kiselev, E. G. Kononova, F. M. Dolgushin, A. S. Peregudov, Y. A. Borisov and V. A. Ol'shevskaya, *Molecules*, 2022, **27**, 7484–7505.
24 J. Singh, S. Lal, R. J. Staples and J. M. Shreeve, *Mater. Chem. Front.*, 2022, **6**, 933–938.
25 M. J. Frisch,G. W. Trucks, H. B. Schlegel, G. E. Scuseria, M. A. Robb, J. R. Cheeseman, G. Scalmani, V. Barone, B. Mennucci, G. A. Petersson, H. Nakatsuji, M. Caricato, X. Li, H. P. Hratchian, A. F. Izmaylov, J. Bloino, G. Zheng, J. L. Sonnenberg, M. Hada, M. Ehara, K. Toyota, R. Fukuda, J. Hasegawa, M. Ishida, T. Nakajima, Y. Honda, O. Kitao, H. Nakai, T. Vreven, J. A. Montgomery, Jr, J. E. Peralta, F. Ogliaro, M. Bearpark, J. J. Heyd, E. Brothers, K. N. Kudin, V. N. Staroverov, R. Kobayashi, J. Normand, K. Raghavachari, A. Rendell, J. C. Burant, S. S. Iyengar, J. Tomasi, M. Cossi, N. Rega, J. M. Millam, M. Klene, J. E. Knox, J. B. Cross, V. Bakken, C. Adamo, J. Jaramillo, R. Gomperts, R. E. Stratmann, O. Yazyev, A. J. Austin, R. Cammi, C. Pomelli, J. W. Ochterski, R. L. Martin, K. Morokuma, V. G. Zakrzewski, G. A. Voth, P. Salvador, J. J. Dannenberg, S. Dapprich, A. D. Daniels, O. Farkas, J. B. Foresman, J. V. Ortiz, J. Cioslowski and D. J. Fox, *Gaussian 09*. Gaussian, Inc., Wallingford, CT, 2009.
26 J. A. Montgomery Jr, M. J. Frisch, J. W. Ochterski and G. A. Petersson, *J. Chem. Phys.*, 2000, **112**, 6532–6542.
27 (*a*) S. J. Blanksby and G. B. Ellison, *Acc. Chem. Res.*, 2003, **36**, 255–263; (*b*) F. Bao, G. Z. Zhang, S. H. Jin, Y. P. Zhang, Q. H. Shu and L. J. Li, *J. Mol. Model.*, 2018, **24**, 85–91.
28 **http://webbook.nist.gov/chemistry/form-ser.html**.
29 P. W. Atkins, *Physical Chemistry*, Oxford University Press, Oxford, 1982.
30 Y. Liu, P. He, L. S. Gong, X. F. Mo and J. G. Zhang, *RSC Adv.*, 2021, **11**, 27420–27430.
31 E. F. Byrd and B. M. Rice, *J. Phys. Chem. A*, 2006, **110**, 1005–1013.
32 F. A. Bulat, A. Toro-Labbé, T. Brinck, J. S. Murray and P. Politzer, *J. Mol. Model.*, 2010, **16**, 1679–1691.
33 T. Lu and F. W. Chen, *J. Comput. Chem.*, 2012, **33**, 580–592.
34 M. J. Kamlet and S. Jacobs, *J. Chem. Phys.*, 1968, **48**, 23–35.
35 P. Politzer, J. Martinez, J. S. Murray, M. C. Concha and A. Toro- Labbé, *Mol. Phys.*, 2009, **107**, 2095–2101.